Kinetic Model for Tensile Deformation of Polymers. 2. Effect of Entanglement Spacing

Yves Termonia*

E. I. du Pont de Nemours and Company, Inc., Central Research and Development Department, Experimental Station, Wilmington, Delaware 19898

Paul Smith

University of California, Materials Department and Department of Chemical and Nuclear Engineering, Santa Barbara, California 93106. *Received October 13, 1987; Revised Manuscript Received January 22, 1988*

ABSTRACT: A new kinetic model for deformation of polymers, introduced previously, is employed to study the orientational and morphological changes that occur during tensile drawing of high molecular weight polyethylene. In the model, the polymer solid is represented by a loose network of entangled chains that are tied together through numerous weak (van der Waals) bonds. The latter represent the crystallinity that provides the initial stiffness to the material. Upon tensile deformation, these bonds are broken, and the chains are deformed and are allowed to slip through entanglements with the help of a Monte Carlo process based on the Eyring chemical activation rate theory. The present study focuses on the effect on the deformation behavior of the entanglement spacing, which can be experimentally varied by using solution crystallization techniques. Calculated stress–strain curves are found to be in excellent agreement with experimental results. Apart from quantitatively predicting the stress–strain behavior, the present model also reveals the various morphological changes that are observed in tensile deformation of polymers.

Introduction

In part 1 of this series, we introduced a new kinetic model for tensile deformation of polymer solids.[1] The model was developed to attempt to quantitatively predict the complete stress–strain behavior of solid polymer materials, including effects of molecular weight distribution, temperature, and strain rate, and to forecast the morphological and orientational phenomena that occur during deformation. This ambitious goal evidently requires that dynamic events on a molecular level are included in the model, such as primary and secondary bond fracture, chain extension, slippage of chains through entanglements, etc. It is the incorporation of these very complex processes that distinguishes the proposed model[1] from the many existing descriptions of polymer deformation. The latter models range from descriptions based on principles of fracture mechanics to static calculations of stress–strain curves of molecular networks and from merely pictorial views to accounts of morphological changes on 10-nm level. (For an exhaustive overview the reader is referred to the excellent text of ref 2). All these models, to our knowledge, are incapable of simultaneously providing quantitative information on (1) stress–strain behavior, molecular extension, chain fracture, and slippage, (2) morphological changes that occur during deformation, and (3) the effects of testing variables, such as temperature and strain rate.

In the preceding part 1[1] we illustrated some of the capabilities of the new model in an investigation of the influence of chain length on the deformation of semicrystalline linear polyethylene (PE). Here we present a study of the important effect of entanglement spacing (i.e., the molecular weight between entanglements) on the deformation of high molecular weight polyethylene. Apart from being academically interesting, this effect has become a topic of industrial significance with the commercialization by DSM/Toyobo and, under licence, Allied Signal Corp. of high-performance polyethylene fibers[3] (sold under the respective trade names Dyneema SK60 and Spectra 900/1000). These fibers are manufactured according to a solution spinning/drawing technique, known as "gel" spinning, which is founded on control of the entanglement spacing through solution processing.

The Model

The model for deformation of polymer solids, briefly presented in ref 1, is described in more elaborate form hereafter.

The undeformed (semi)crystalline polymer solid is represented by a loose network of entangled macromolecules. Prior to deformation, the chain strands between the entanglement loci are coiled and are tied together through weak inter- and intramolecular bonds, e.g., van der Waals forces. These forces represent the initial stiffness to the polymer. This representation of the polymer solid is illustrated in the schematic of Figure 1a. The heavy black circles in this figure denote the entanglement loci. The dotted lines represent the weak attractive (van der Waals) bonds connecting sections either of the same chain or of different chains. Since the coordination number of an entanglement is assumed to be 4, the actual three-dimensional network for convenience has been given a planar (x–y) configuration. The y axis is chosen as the direction of draw. Periodic boundary conditions are imposed along the transverse x axis.

In the present model, the above polymer solid is further simplified as shown in Figure 1b. Here, the details of the chain configurations are omitted altogether. The coiled chain strands between entanglements are replaced by chain vectors denoted by heavy solid lines. Chain strands that do not connect two entanglement loci (i.e., chain end sections) are indicated by shorter solid lines. In actual undeformed solids the chain vectors are randomly oriented in three-dimensional space, i.e., $\langle \cos^2 \theta \rangle = {}^1/_3$, where θ is the vector's angle with the draw axis. Accordingly, in our two-dimensional lattice representation of Figure 1b we take the value $\theta = 54.7°$ for all vector orientations along the draw (y) axis.[4] The various van der Waals (vdW) bonds are replaced by "overall" bonds (dotted lines in Figure 1b) joining each entanglement point to its neighbors. Only overall bonds between the two nearest neighbors are taken into account.

The entanglement lattice in the present work is filled in with macromolecules of monodisperse molecular weight M. This is a rather complex operation that is realized as follows. For given values of M and M_e (the molecular

0024-9297/88/2221-2184$01.50/0

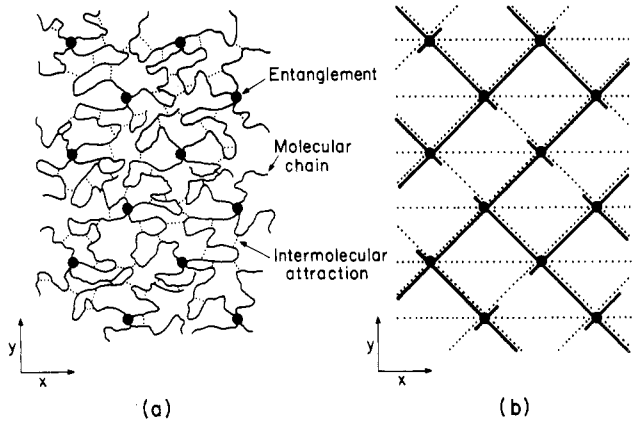

Figure 1. (a) Dense system of polymer chains. The heavy black circles represent entanglement loci, and the dotted lines denote the van der Waals bonds. (b) More schematic representation of the network in a. The heavy solid lines indicate chain vectors between entanglements; chain ends are represented by shorter solid lines. Individual vdW bonds have been replaced by "overall" bonds (dotted lines) joining each entanglement to its nearest neighbors.

weight between entanglements) random chains of M/M_e strands are constructed by using a step-by-step procedure based on examining—at each step—for possible continuations of the chain in the subsequent steps.[5] This procedure allows to fill in the lattice with macromolecules of a length distribution as close as possible to monodisperse.

This macromolecular network is deformed at constant temperature and a rate of elongation $\dot{\epsilon}$. This leads to straining of the van der Waals bonds, which are broken, according to the Eyring kinetic theory of fracture,[6] at a rate

$$\upsilon = \tau \exp[-(U - \beta\sigma)/kT] \quad (1)$$

In eq 1, τ is the thermal vibration frequency, U and β are, respectively, the activation energy and volume whereas

$$\sigma = \kappa\epsilon \quad (2)$$

is the local stress. Here, σ is the local strain and κ is the elastic constant of the bond. These vdW bond breakages lead to a release of the chain strands, which are now to support the external load. Once broken, vdW bonds are assumed not to reform. The present model thus ignores the possible influence of the crystalline phase in the deformation process past its initial stage. Experimental evidence has accumulated[7] that plastic deformation of weakly bonded polymer systems is dominated not by crystallites but by chain entanglements; this justifies the present simplification.

As the stress on the "freed" chain strands increases, slippage through entanglements is assumed to set in at a rate that has the same functional form as that for vdW breakings (eq 1) but with different values for the activation energy U and volume β. σ now denotes the difference in stress in two consecutive chain strands that are separated by an entanglement. This stress difference is calculated by using the classical treatment of rubber elasticity.[8] According to this theory, the stress on a stretched chain strand having a vector length $\mathbf{r}$ is given by

$$\sigma = \alpha kT\, L^{-1}(\mathbf{r}/nl) \quad (3)$$

Here n is the number of statistical chains segments[9] of length l in a strand. L^{-1} is the inverse Langevin function, and α is a proportionality constant that depends on the number N of chain strands per unit volume. Following Treloar[8]

$$\alpha = (N/3)n^{1/2} \quad (4)$$

In accordance with reported experimental data for viscous flow of paraffins,[10] we assume the average length of a hydrocarbon chain capable of a coordinated movement, at a rate given by eq 2, is approximately 25 carbon atoms. This slippage process leads to a change in the number of statistical chain units between entanglements and, occasionally, to chain disentanglement. If the rate of chain slippage is very low, maximum elongation of the chain strands between entanglements can be reached, and chain fracture occurs at a local draw ratio $\lambda = n^{1/2}$. In view of the high stresses required for chain rupture and the ensuing important retraction of the broken molecular ends, fractured chains are assumed not to reform.

Simulation

The kinetic model described above is simulated (using techniques similar to those employed in our studies of the maximum theoretical strength of polymer fibers[11]) on an $(x-y)$ array of up to 60×120 entanglement loci.

The simulation of the vdW bond breakings is performed with the help of a Monte Carlo lottery which breaks a bond i according to a probability

$$p_i = \upsilon_i/\upsilon_{max} \quad (5)$$

where υ_{max} is the rate of breakage of the most strained bond in the array. After each visit of a bond, the "time" t is augmented by $1/[\upsilon_{max}\, n(t)]$ where $n(t)$ is the total number of intact bonds at time t. As was mentioned above in the description of the present model, broken vdW bonds are assumed not to reform.

Simulation of chain slippage through entanglements is executed by using a similar technique. Now $n(t)$ denotes the total number of entanglements left at time t. After a very small time interval δt has elapsed, the vdW bond breaking, chain slippage, and fracture processes are halted, and the network is elongated along the y axis by a small constant amount that is determined by the rate of elongation $\dot{\epsilon}$. Subsequently, the whole network is relaxed to its minimum energy configuration. This relaxation is executed by using a series of fast computer algorithms, described in ref 11, which steadily reduce the net residual force acting on each entanglement point. This leads to displacements of the entanglement loci along the x and y axes.[12] To save computer time, only displacements along the draw axis are explicitly calculated. Distances in the transverse x direction are assumed to be contracted homogeneously by a factor $\lambda^{-1/2}$, where λ is the overall draw ratio along the y axis.[13] After these relaxation steps, which constitute the most computer-time-consuming processes in the simulation, the axial nominal stress at one end of the network is calculated. The Monte Carlo process of bond breakings and chain slippage is then restarted for another time interval δt, and so on and so forth, until the network fails.

Results and Discussion

The model has been applied to study the tensile deformation behavior of solid, linear polyethylene. In part 1 of this series[1] we reported on the effect of the molecular weight; here, we explore the influence of the entanglement spacing at constant molecular weight. Detailed studies on the important effects of temperature, rate of deformation, molecular weight distribution, etc., will be reported in subsequent papers.

Parameters. The following values of the various parameters in the model were employed:

A *statistical chain segment* of polyethylene has a molecular weight of about 140 and a length of approximately $l = 10$ Å.[9] The atomic vibration frequency is taken to be

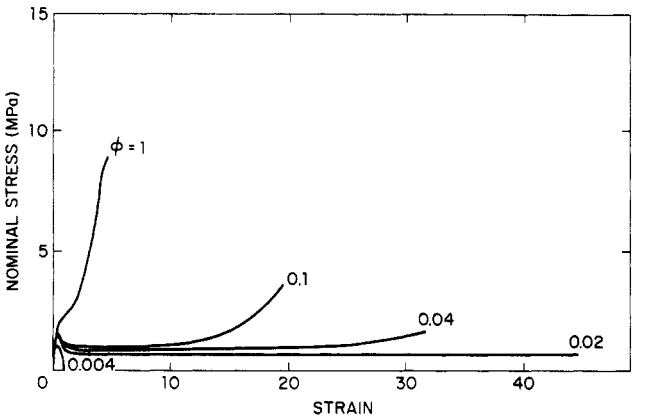

Figure 2. Calculated nominal stress–strain curves for monodisperse linear polyethylene with M = 475 000, at four different values, indicated in the graph, of the entanglement spacing factor ϕ (see text). The deformation temperature was 109 °C, and the rate of elongation was 500%/min.

10^{12}/s, independent of the temperature. A rate of elongation $\dot{\epsilon}$ = 5/min was selected. Values for the other parameters (eqs 1–4) are as follows:

vdW Bond Breakage. The elastic modulus κ was taken to be 4 MPa.[1] We chose U = 30 kcal/mol, which equals the activation energy necessary to break 20–30 vdW bonds. Concomitantly, we took β = (26 Å)^3.[1]

Chain Slippage. The number N of chain strands per unit volume (eq 4) is given by

$$N = \rho/M_e \tag{6}$$

where the density ρ was taken to be 1000 kg/m^3. The activation energy U = 20 kcal/mol, and the activation volume β = (7 Å)^3.[1] The latter value is of the order of magnitude of the volume of a statistical chain segment and is consistent with the commonly accepted idea (ref 10 and note below eq 4) that slippage involves the coordinated movement of one to two statistical chain segments, at most.

Entanglement Spacing. To systematically examine the effect on the deformation behavior of the entanglement spacing, i.e., of the number of statistical chain segments between entanglements, we introduce the spacing factor ϕ defined as

$$\phi = (M_e/1900)^{-1} \tag{7}$$

The numerical scaling factor 1900 is, in fact, the approximate molecular weight between entanglements in melts of linear polyethylene macromolecules;[14] it corresponds to about 14 statistical chain segments. The selection of the spacing factor ϕ is, of course, not coincidental. It is well-known that entanglements can be spaced apart experimentally through dilution of the polymer. The molecular weight between entanglements in solution is approximately given by the relation

$$(M_e)^{soln} \sim (M_e)^{melt}/\phi \tag{8}$$

where ϕ is the volume fraction of the polymer.[15] In this work we, therefore, employed $\phi = (M_e)^{melt}/(M_e)^{soln}$ as the entanglement spacing factor. This choice permitted us to readily examine the results of the present calculations against experimental data on the deformation behavior of solution-crystallized, or "gel-spun", polyethylene.

Stress–Strain Curves. Figure 2 shows a series of nominal stress–strain curves calculated for monodisperse polyethylene of M = 475 000 at five different values of the entanglement spacing factor ϕ (1, 0.1, 0.04, 0.02 and 0.004). The deformation temperature was taken to be 109 °C. This figure reveals the dramatic effect of the entanglement

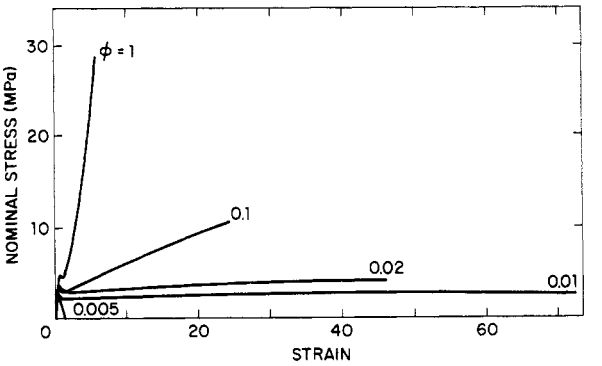

Figure 3. Experimental stress–strain curves recorded at 120 °C for ultrahigh molecular weight (UHMW) polyethylene films (M_w = 1.5 × 10^6, M_n ~ 2 × 10^5) crystallized from the melt and from solutions of various initial polymer concentrations: 10, 2, 1, and 0.5% by volume of the polymer. Prior to deformation, the solvent had been removed from these films to reveal only the effect of the initial polymer volume fraction and to eliminate possible plasticizing effects of the solvent (see ref 7 for further experimental details).

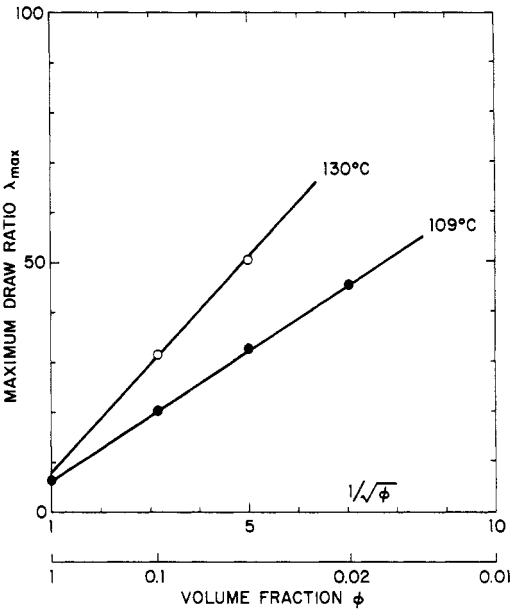

Figure 4. Calculated maximum draw ratios (strain at break + 1) plotted versus (the entanglement spacing factor)$^{-1/2}$ at deformation temperatures of 109 and 130 °C.

spacing on the deformation characteristics, notably on the postyield strain hardening, and on the strain at break. At decreasing values of ϕ, the rate of strain hardening, i.e., the postyield modulus, rapidly dropped to reach a negative value at ϕ = 0.004. The strain at break, on the other hand, drastically increased from 4.5 to 45 when ϕ decreased from 1 to 0.02. At much lower values of ϕ, e.g., 0.004, the plastic deformation leading to high values of the strain at break no longer occurred as a result of continued strain softening and ductile failure was observed. The latter result is, of course, due to the fact that at ϕ = 0.004 the molecular weight between entanglements is 1900/0.004 = 475 000, which equals the molecular weight of the polyethylene in the simulation. Accordingly, transfer of applied load, in this special case, occurs only from one chain to its nearest neighbors through weak vdW bonds, and stress concentrations arising from vdW bond breaks are not distributed uniformly throughout the entanglement network. As a result, very little deformation occurred and failure was highly localized (see also the morphology in Figure 5a).

The calculated stress–strain curves of Figure 2 show a remarkably good accord with those recorded of ultrahigh

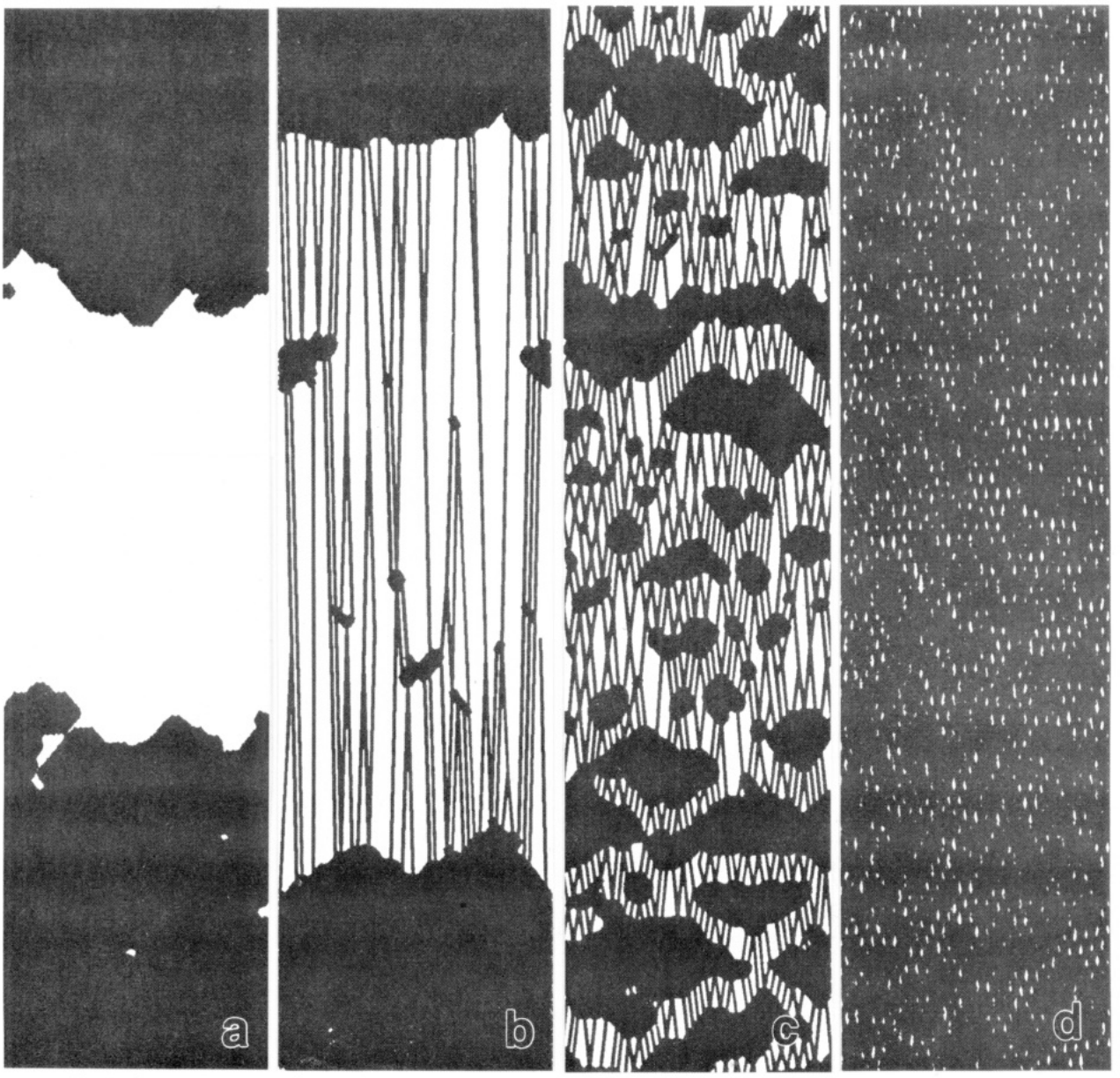

Figure 5. Typical "morphologies" obtained with the model for the materials of Figure 2 with ϕ: (a) −0.004; (b) −0.02; (c) −0.1; (d) −1. In cases b–d the draw raio $\lambda = 2.7$. The widths of the "samples" are respectively 3.2, 1.6, 0.7, and 0.2 μm.

molecular weight (UHMW) polyethylene crystallized from solutions of various initial polymer concentrations.[7] For comparison purposes, these—previously reported—experimental results are reprinted in the graph of Figure 3. This graph displays stress–strain curves, recorded at 120 °C of UHMW films ($M_w = 1.5 \times 10^6$, $M_n \sim 2 \times 10^5$) derived from the melt and from solutions that contained respectively 10, 2, 1, and 0.5% by volume of the polymer. Prior to deformation, the solvent had been removed from these films to reveal only the effect of the initial polymer volume fraction and to eliminate possible plasticizing effects of the solvent (see ref 7 for further experimental details). In the same work it was reported that polyethylene solids produced from a 0.5% solution exhibited continued strain-softening, which is in gratifying accord with the present calculations.

The systematic increase of the strain at break, or rather of the maximum draw ratio λ_{max}, of solution-crystallized UHMW PE observed in the experimental study cited above was found to obey the simple relation

$$\lambda_{max} \propto \phi^{-1/2} \tag{9}$$

This relation finds its origin in the combined dependence of the draw ratio on the square root of the number of statistical chain segments between entanglements and the concentration dependence (eq 8) of the latter (see ref 7).

Figure 4 shows the calculated maximum draw ratios (strain at break + 1) plotted versus $\phi^{-1/2}$. The perfectly linear correlation between λ_{max} and $\phi^{-1/2}$ clearly favors this −0.5 power law exponent over the recently proposed[16] value of −0.83, which was derived from swelling equilibrium considerations. The slope of the curve in Figure 4 equals 6.4, which indicates that virtually no removal of entanglements through chain slippage had occurred during the deformation at 109 °C. In the absence of slippage, i.e., in the case of affine deformation, this proportionality factor has the value of $14^{1/2} \times 3^{1/2} = 6.5$.[7,17,18] In separate studies (to be published elsewhere) on the effect of temperature on the deformation behavior, it was found that chain slippage, which leads to higher values of this factor, becomes exceedingly relevant at temperatures in excess of 115 °C; that is for molecular weights of the order of 500 000. This is, in fact, illustrated in Figure 4, which shows the substantially higher maximum draw ratios at

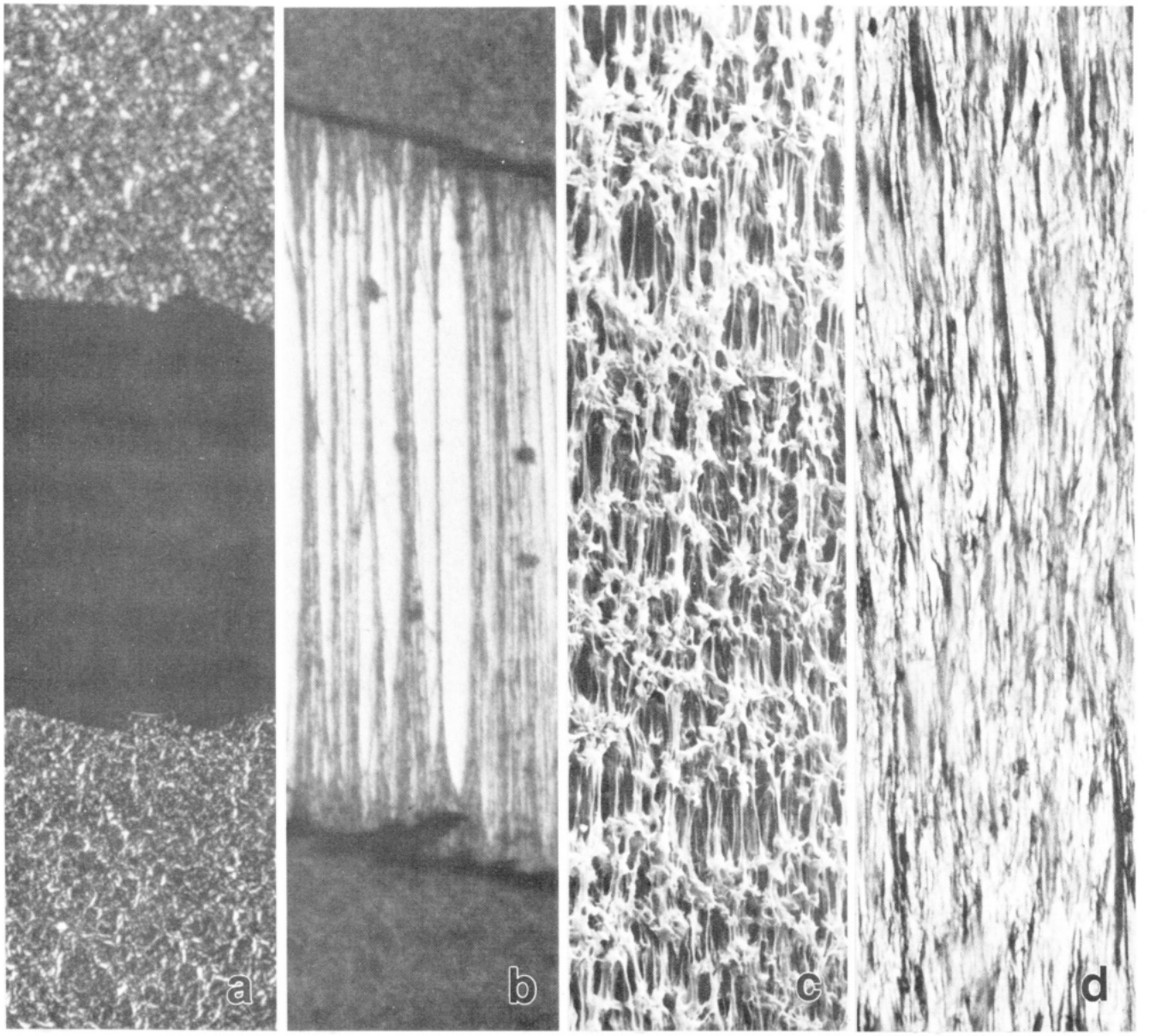

Figure 6. Micrographs of drawn samples of polyethylene films of $M_w = 1.5 \times 10^6$ and $M_n \sim 2 \times 10^5$ crystallized from solutions in Decalin and from the melt (see ref 19 for experimental details); these samples were drawn to a macroscopic draw ratio of approximately 3 at 100 °C. The initial polymer volume fractions were respectively (a) $-\phi = 0.005$; (b) $-\phi = 0.02$; (c) $-\phi = 0.1$; (d) $-\phi = 1$. Prints a, b, and d are optical micrographs taken under crossed polarizers (except b), and c is a scanning electron micrograph. The width of all strips shown is 0.1 mm.

a deformation temperature of 130 °C.

By comparing the experimental data presented in Figure 3 and the calculated results displayed in Figure 2, it is clear that the current model predicts very well the dramatic effect of the initial polymer volume fraction on the deformation behavior of UHMW PE, particularly the spectacular increase of the strain at break at decreasing polymer concentration. Originally, this effect was explained in terms of reduced entanglement densities in solution-crystallized polymer solids.[7] The present calculations, which are based on this concept, of course, strongly reinforce this hypothesis. In turn, the excellent agreement between calculated and measured stress–strain curves provides great confidence in the model.

There are a some differences to be noted between the calculated and experimental stress–strain curves. Generally, the predicted stress levels are below the experimentally observed values. This is due to our totally neglecting the contributions of the crystalline phase to the plastic deformation process.[1] In our opinion, a more important difference is the upswing, or strain hardening, found in most of the calculated stress–strain curves prior to reaching the strain at break. This "upswing" has not been observed experimentally, except for melt-crystallized UHMW PE. At this point, it is not clear whether this feature is due to the fact that the calculations were carried out for monodisperse chain molecules, which is unlike the polymer employed in the experiments. An exhaustive analysis of the major effects of molecular weight distribution on the deformation behavior is forthcoming.

Morphology. It was pointed out in the Introduction that the present model also provides schematic "morphologies" of the deformed polymer solids by plotting the positions of the entanglement loci and the connecting chain vectors. Figure 5 shows these morphologies for four entanglement spacing factors $\phi = 1$, 0.1, 0.02, and 0.004, at an "overall" draw ratio of 2.7 (except for $\phi = 0.004$). This figure displays the dramatic effect of the entanglement spacing on the fractography, the deformation behavior and particularly the necking phenomena. At the

very low value of $\phi = 0.004$ brittlelike fracture was observed. At the higher value of 0.02 a well-defined neck appeared, which upon subsequent deformation traveled through the entire specimen. For $\phi = 1$ essentially homogeneous deformation was observed, whereas $\phi = 0.1$ represents an intermediate case between homogeneous deformation and necking. In the latter case multiple micronecks were formed.

It was already noted above that the morphologies generated with the model are unrealistically porous in highly deformed regions. And it was explained[13] that this is a direct consequence of the simplification (to save computer time) that the specimen was contracted along the x axis by the square root of the overall draw ratio, instead of local draw ratio. The latter, of course, may differ widely from the overall draw ratio, particularly in materials with a low value of ϕ. This discrepancy is clearly illustrated in Figure 5b,c.

For purpose of comparison, micrographs of actual samples of solution-crystallized UHMW PE are presented in Figure 6. This figure displays photographs of polyethylene films of $M_w = 1.5 \times 10^6$ and $M_n \sim 2 \times 10^5$ crystallized from respectively 0.5, 2, and 10% v/v solutions in Decalin and from the melt (see ref 19 for experimental details); the latter three samples were drawn to a macroscopic draw ratio of approximately 3 at 100 °C. The resemblance between these micrographs and the "calculated morphologies" of Figure 5 is truly remarkable. It illustrates that the present model indeed is capable of handling the very complex issue of connecting events on molecular level to macroscopic properties and features.

Acknowledgment. We thank Dr. S. R. Allen for many stimulating discussions and Dr. E. J. Roche for producing the optical micrographs.

Registry No. PE, 9002-88-4.

References and Notes

(1) Termonia, Y.; Smith, P. *Macromolecules* **1987**, *20*, 835.
(2) Ward, I. M. *Mechanical Properties of Solid Polymes, 2nd ed.*; Wiley: New York, 1983.
(3) Smith, P.; Lemstra, P. J. to Stamicarbon, B. V. (DSM), U.S. Patent 4 344 908, 1982; U.S. Patent 4 430 383, 1983.
(4) In contrast to studies based on the affine deformation principle, the importance of the initial distribution of orientations along the deformation axis here is of little importance. Indeed, in the present approach, that distribution is destroyed already in the early stages of the deformation process after a few van der Waals bond breakings or slippage events have occurred (see below).
(5) Meirovitch, H. *J. Phys. A: Math. Gen.* **1982**, *A15*, L735; *J. Chem. Phys.* **1983**, *79*, 502.
(6) See, e.g., the review in: Kausch, H. H. *Polymer Fracture*; Springer-Verlag: Berlin, 1978; Chapter IV.
(7) Smith, P.; Lemstra, P. J.; Booij, H. C. *J. Polym. Sci., Polym. Phys. Ed.* **1981**, *19*, 877.
(8) Treloar, L. R. G. *The Physics of Rubber Elasticity*, 2nd ed.; Clarendon: Oxford; 1985.
(9) Flory, P. J. *Statistical Mechanics of Chain Molecules*; Interscience: New York, 1969; p 12.
(10) Kauzmann, H.; Eyring, H. *J. Am. Chem. Soc.* **1940**, *62*, 3113.
(11) Termonia, Y.; Meakin, P.; Smith, P. *Macromolecules* **1985**, *18*, 2246; *Ibid* **1986**, *19*, 154.
(12) During that process the end-to-end vectors of chain strands are prohibited to contract below their equilibrium length corresponding to the random coil configuration.
(13) This calculation is an oversimplification that ignores the fact that locally the draw ratios may be very large indeed, and this procedure thus undercompensates for contractions along the x axis. This leads to too large distances between the chains in the x direction and to too "open" a morphology (see later). This simplification, which amounts to an important saving in computer time, is justified because the principal axis of interest in the present work is the y axis.
(14) Porter, R. S.; Johnson, J. F. *Chem. Rev.* **1966**, *66*, 1.
(15) Graessley, W. W. *Adv. Polym. Sci.* **1974**, *16*, 58.
(16) Mackley, M. R.; Solbai, S. *Polymer* **1987**, *28*, 1115.
(17) In the paper of ref 7, where relation 9 originally was proposed, the factor $3^{1/2}$ was erroneously omitted (see ref 18).
(18) Kramer, E. J. *Adv. Polym. Sci.* **1983**, *52/53*, 33.
(19) Smith, P.; Lemstra, P. J.; Pijpers, J. P. L.; Kiel, A. M. *Colloid Polym. Sci.* **1981**, *259*, 1070.

Effect of Chain Association on the Viscosity of Dilute Ionomer Solutions

Fumihiko Tanaka

Laboratory of Physics, Faculty of General Education, Tokyo University of Agriculture and Technology, Fuchu-shi, Tokyo 183, Japan. *Received September 24, 1987; Revised Manuscript Received December 21, 1987*

ABSTRACT: Ionic groups attached at wide intervals along nonpolar polymer chains produce strong associating interactions in solution. This paper presents a general theory to infer the detailed structure of chain aggregates from the experimental data on the solution viscosity of ionomers in nonpolar solvents. In the limit of low concentration, equilibrium dimensions of an intramolecular network formed by ionic interaction are estimated as a function of χ (the solvent–monomer interaction parameter) and ϵ (strength of the bonding energy). For higher polymer concentrations, cluster distribution function of intermolecular aggregates is obtained through multiple-equilibria conditions. It is shown that their geometrical structure is characterized by two exponents, q and ν, giving interchain connectivity and fractal dimensionality, respectively. The result is compared with the recent experimental measurements on sodium sulfonated polystyrene in cyclohexanone.

I. Introduction

Flexible long-chain molecules containing a small fraction of strongly associating chemical groups are known to exhibit several unusual solution properties. For example, the incorporation of relatively low levels of ionic groups onto the backbone structure of a polymer chain profoundly changes the rheological properties of these solutions as compared to its nonionic counterpart. These changes are caused to a large extent by the formation of intra- and intermolecular cross-links due to the mutual association of the ionic groups.

Recent experimental studies[1-3] have explored the solution viscosity of polymers such as sulfonated polystyrene ionomers or ethylene–propylene terpolymers over wide

0024-9297/88/2221-2189$01.50/0